

## Strongly dipolar fluids at low densities compared to living polymers

J. M. Tavares,<sup>1</sup> J. J. Weis,<sup>2</sup> and M. M. Telo da Gama<sup>1</sup>

<sup>1</sup>*Departamento de Física da Faculdade de Ciências and Centro de Física da Matéria Condensada, Universidade de Lisboa, Avenida Professor Gama Pinto 2, P-1649-003 Lisboa Codex, Portugal*

<sup>2</sup>*Laboratoire de Physique Théorique et Hautes Energies,\* Université de Paris XI, Bâtiment 211, F-91405 Orsay Cedex, France*

(Received 5 November 1998)

We carried out extensive canonical Monte Carlo (MC) simulations of the dipolar hard-sphere (DHS) fluid, with  $N=1024$  particles at fixed reduced density  $\rho^*=0.05$ , in order to investigate the chainlike structure that occurs at low densities, for sufficiently large reduced dipole moments  $\mu^*$ . The dissociation and recombination of chains during equilibrium runs suggest an analogy between the DHS's and a system of living polymers. This was checked quantitatively by comparing the results of the simulations with those of a theory for living polymers taking into account the indistinguishability of the particles in self-assembled chains. Quantitative agreement between theoretical and simulated mean chain lengths and number of monomers, was found for particular choices of the parameters used in the working definition of the MC chains.

PACS number(s): 61.20.Gy, 61.20.Qg, 61.41.+e

### I. INTRODUCTION

In recent years there has been renewed interest in the thermodynamic and structural properties of dipolar fluid models, hard (DHS) or soft spheres with an embedded point dipole. Numerical simulations revealed an entirely new behavior, not predicted by existing theories: formation of chainlike structures for strongly dipolar fluids (with [1–3] or without [4,5] an applied magnetic field) at low densities, appearance of a ferromagnetically ordered fluid phase [6,7] and absence of liquid-vapor condensation unless external magnetic fields [1,3] or isotropic interactions between spheres are considered [8]. Various theoretical approaches were proposed to investigate these new features: integral equations [9] and density-functional theory [10] were used to describe the ferromagnetic fluid phase, and models for associating fluids, treated within mean field approximations, were used to describe the absence of condensation of DHS and the onset of chain formation at low densities [11–13].

The simulations of strongly dipolar fluids, at low densities, revealed that the spheres associate into linear chainlike structures, that grow or shrink as the dipole moment increases or decreases. Moreover, it was shown that the chains break up and recombine in the course of equilibrium simulation runs [4], suggesting that the system behaves as a system of living polymers. As the spatial and orientational many-body correlations that describe these aggregates cannot be calculated directly during a simulation run, an alternative description of the structure was proposed in [4,5] and [1,2], by defining an (off-lattice) “living” chain based on an energetic criterium: two spheres belong to a chain if their interaction energy is lower than a given threshold. For each equilibrium configuration it is then possible to determine the

number of chains of a given length and then the equilibrium chain length distribution, the mean chain length, etc., are calculated easily by performing the appropriate averages.

A similar approach was taken by [12] that considers the low-density DHS fluid as a system of (independent) self-assembled chains, with a free energy that corresponds to that of an ideal mixture of chains of all lengths. The chains are formed by dipolar hard spheres with a bonding energy given by the minimum of the dipolar pair potential (touching spheres with dipoles aligned “head to tail”). The mean chain length was calculated as a function of the density and dipole moment (or temperature) and compared with simulation results. The comparison suggested qualitative agreement for the exponential growth of the mean chain length with increasing dipole moment (or decreasing temperature). It was argued in [12] that the large discrepancies found in some cases were due to finite size effects of the simulation and/or lack of equilibration for systems with the strongest dipole moments.

In this work we carry out the comparison between theoretical and simulation results in more detail. In Sec. II, we describe Monte Carlo (MC) simulations of DHS for a system with 1024 particles and reduced density,  $\rho^*=0.05$ . We have performed longer runs to ensure that equilibrium is reached even for systems with the strongest dipoles (lowest temperatures). The definition of a MC chain required in the analysis of the simulation results is discussed in detail. In Sec. III, we apply the theory of living polymers to the DHS fluid, improve on some of the results of [12] and compare the theoretical and simulation results. We make some concluding remarks in Sec. IV.

### II. SIMULATIONS

We consider a system of hard spheres with radius  $\sigma$  and embedded dipoles of strength  $\mu$ , interacting through the pair potential,

\*The Laboratoire de Physique Théorique et Hautes Energies is associé au Centre National de Recherche Scientifique (No. URA 0063).

TABLE I. Details of the simulation runs.  $U$  is the dipolar internal energy calculated through the Ewald sum.  $NEC$  is the number of equilibrium configurations stored to analyze the structure.  $\mu^*$ ,  $\rho^*$  and  $N$  are defined in the text.

$\mu^*$	$N$	$\rho^*$	trial moves/N	$\beta U/N$	$NEC$
2.25	1024	0.05	172 000	-6.59	344
2.5	1024	0.05	222 500	-10.70	445
2.75	1024	0.05	260 000	-14.38	520

$$\phi_{DHS} = \begin{cases} \infty, & r_{12} < \sigma \\ -\frac{\mu^2}{r_{12}^3} [3(\hat{\mu}_1 \cdot \hat{r}_{12})(\hat{\mu}_2 \cdot \hat{r}_{12}) - \hat{\mu}_1 \cdot \hat{\mu}_2] & r_{12} \geq \sigma. \end{cases} \quad (1)$$

$r_{12}$  is the distance between the centers of spheres,  $\hat{r}_{12}$  the unit interdipolar vector, and  $\hat{\mu}_1$  and  $\hat{\mu}_2$  the unit dipolar vectors of spheres 1 and 2, respectively. Canonical MC simulations are carried out for a system with  $N=1024$  spheres (twice the largest number used in previous simulations of this model), at fixed reduced density  $\rho^* \equiv \sigma^3 \rho = 0.05$ , for several values of the reduced dipole moment (or square root of the inverse reduced temperature) defined as

$$\mu^* = \left( \frac{\mu^2}{k_B T \sigma^3} \right)^{1/2}. \quad (2)$$

$k_B$  is Boltzmann's constant and  $T$  the absolute temperature.

Each MC step consists of the attempt of simultaneously moving a sphere and rotating its dipole. The maximum displacement and angles of rotation were chosen to ensure an acceptance ratio of  $\sim 40\%$ . Systems were equilibrated with 20 000–30 000 MC trials. To accelerate equilibration we used, when possible, the last equilibrium configuration for a given dipole moment  $\mu^*$ , as the initial configuration for the simulation with the next  $\mu^*$ . The equilibration process was controlled by inspection of the internal energy. To handle the long-range dipolar forces we used the Ewald sum technique exactly as in [6], where details can be found. Surface effects were included through an infinite dielectric constant (surrounding conducting medium, see [6]), although, at this density, the system is not expected to be polarized and thus this effect is negligible.

The goal of the new simulations is the systematic study of chain formation at low reduced density, as a function of the dipole moment  $\mu^*$ . We performed preliminary (short) simulations for values of  $\mu^*$  in the range 1.5–3. These indicated that self-assembly starts at  $\mu^* \approx 2$  and chains with lengths similar to that of the simulation box appear often, when  $\mu^* = 3$ . Thus we chose  $\mu^* = 2.25, 2.5, 2.75$  to perform longer simulations to investigate the structural properties of the system. We avoided higher values of the dipole moment to minimize finite size effects that cannot be neglected when chains become as long as the linear dimension of the simulation box. Table I summarizes the details of the simulation runs. Note the number of MC steps after equilibration that is much larger than that of earlier works (e.g., [5]).

The dipole-dipole potential (1) has a global minimum when the dipoles of two spheres at contact are aligned head to tail. It is expected that, at sufficiently high dipole moments, this structure reveals itself, at least locally. Indeed, snapshots of equilibrium configurations [4] show that dipolar spheres self-assemble forming linear structures that may span the simulation box, indicating that the dipole-dipole potential induces strong many-body spatial and angular correlations, at low density and temperature (large reduced dipole moment).

A direct calculation of these many-body correlations is not feasible in a simulation or theoretically. An approximate approach that is useful both in the analysis of the simulation results and in the construction of a theoretical description has been used, by advancing the hypothesis (based on the analysis of simulation results [4]) that these correlations are described rather accurately by the size distribution function of an assembly of chains [1,2,4,5,11,12]. The equilibrium structure of the system is then given in terms of the thermal distribution of chain lengths.

In [1,2,4,5] chains were defined as follows. For a given equilibrium (MC) configuration, the lowest ( $E_1^i$ ) and second lowest ( $E_2^i$ ) energies of interaction of each particle ( $i$ ) are calculated; if both energies are above a certain threshold  $E_c$ , the particle is a (“free”) monomer. Otherwise the particle is in a chain, being at one of the ends if only  $E_1$  is less than  $E_c$ .

In [4,5] this procedure was implemented for a set of equilibrium configurations yielding the description of the structure in terms of the thermal distribution of chain lengths. The mean chain length and the number of “free” monomers are calculated from the equilibrium distribution. As we will see these results depend on the threshold energy,  $E_c$ . In [4,5] the threshold was set to  $E_c = -1.4\mu^{*2}$ , a value suggested by the analysis of the mean values of  $E_1^i, E_2^i$ , and  $E_3^i$  (the third lowest energy of interaction) for several equilibrium configurations. Aggregation into chains occurs if the mean values of  $E_1^i$  and  $E_2^i$  are close to each other and much lower than the mean value of  $E_3^i$ . Stevens and Grest, however, chose  $E_c = -0.5\mu^{*2}$  in [1]. The effect of this choice on the structural parameters of the system (mean chain length, number of monomers, etc.) was not considered by these authors.

We define the functions,  $N_1(E), N_2(E)$ , and  $N_3(E)$ , as the number of particles with first, second, and third lowest energies of interaction in the energy interval  $[E-dE; E+dE]$ . These functions are defined in  $]-2\mu^{*2}; +\infty[$  and normalized,

$$N = \int_{-2\mu^{*2}}^{\infty} N_i(E) dE. \quad (3)$$

The number of free monomers  $N_m$  is the number of particles with lowest energy of interaction greater than  $E_c$ ,

$$N_m = \int_{E_c}^{\infty} N_1(E) dE. \quad (4)$$

If  $\rho$  is the total density of spheres, the density of free monomers is  $\rho_1 = (N_m/N)\rho$ . The number of chains ( $N_{ch}$ ) is half the number of particles at the end of chains ( $N_{ec}, N_{ch}$

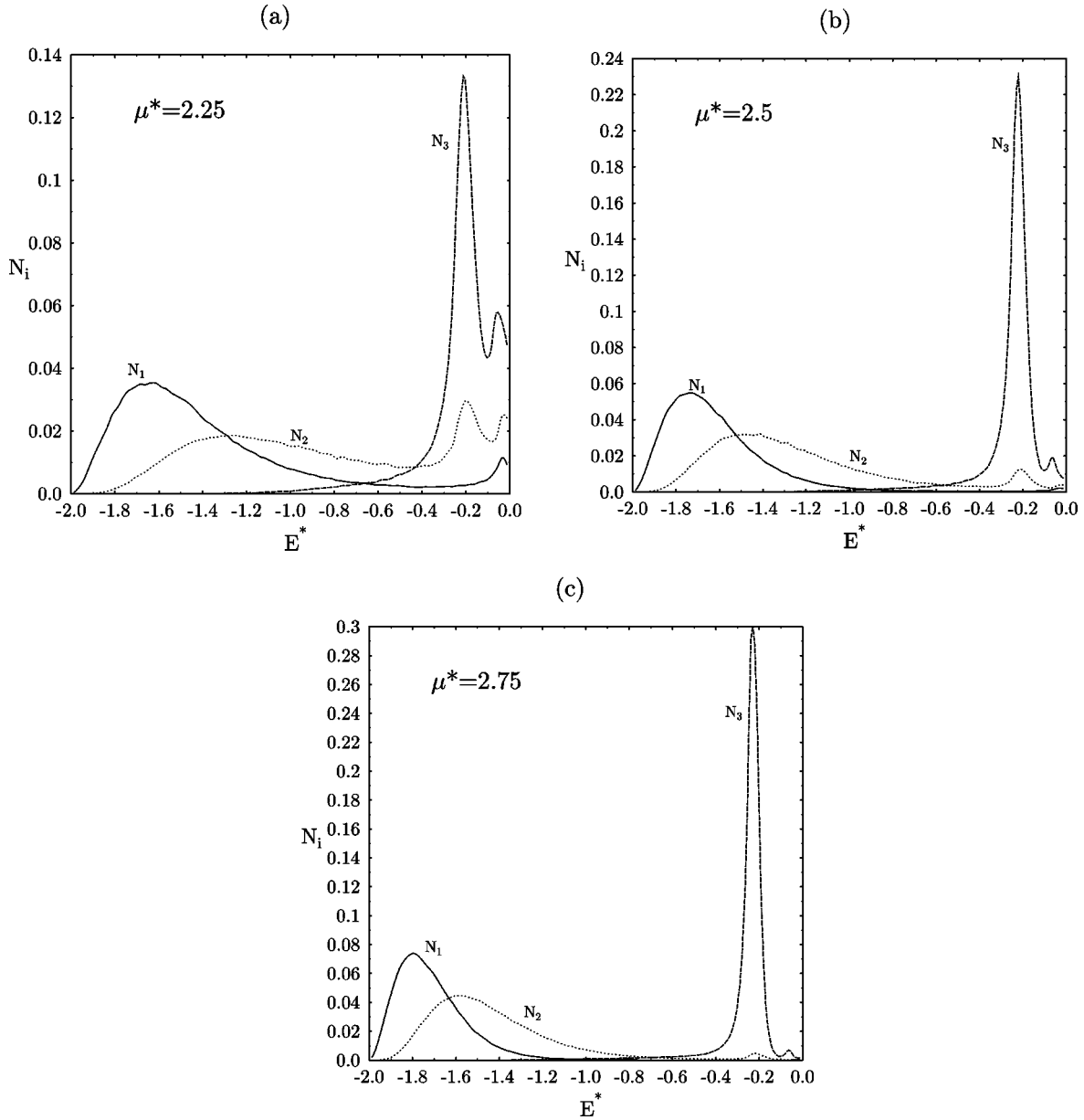


FIG. 1. Functions  $N_1, N_2$ , and  $N_3$  for the simulated systems.  $E^* = E/\mu^{*2}$ . (a)  $\mu^* = 2.25$ , (b)  $\mu^* = 2.5$ , (c)  $\mu^* = 2.75$ .

$=N_{ec}/2$ . A particle is at the end of a chain if its lowest energy of interaction (but not its second lowest) is less than  $E_c$ , and thus

$$N_{ch} = \frac{N_{ec}}{2} = \frac{1}{2} \int_{-2\mu^{*2}}^{E_c} [N_1(E) - N_2(E)] dE. \quad (5)$$

Finally the number of monomers in the middle of chains  $N_{mc}$  is given by

$$N_{mc} = \int_{-2\mu^{*2}}^{E_c} N_2(E) dE. \quad (6)$$

The mean chain length  $\bar{N}$  is the ratio of the total number of particles and chains, including chains of length 1, i.e., free monomers [4,12],

$$\bar{N} = \frac{N}{N_m + N_{ch}}. \quad (7)$$

$N_1(E), N_2(E)$ , and  $N_3(E)$  were obtained from the simulation of systems with  $\mu^* = 2.25, 2.5$ , and  $2.75$  [Figs. 1(a)–1(c)] as follows. The interval  $[-2\mu^{*2}; 0]$  is divided into 80 subintervals of equal length centered at  $E_k (k = 1 \dots 80)$ ; for each equilibrium configuration the lowest, second, and third lowest energies of interaction of each particle were determined and histograms  $N_i(E_k)$  were calculated and averaged over all configurations.

The structure of the fluid is chainlike, if most of the particles have nearest (all particles except free monomers) and second nearest (all particles except free monomers and particles at the end of chains) neighbors with energies close to  $-2\mu^{*2}$ , which is clearly illustrated in Figs. 1(a)–1(c). An increase of the fraction of particles in chains with increasing dipole moment is evident in these figures, where the maxima

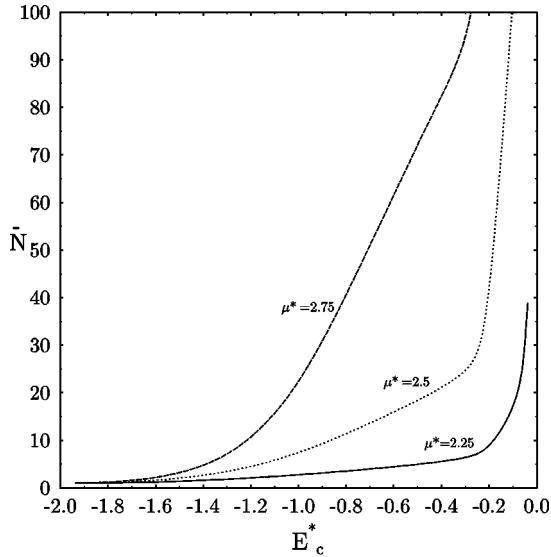


FIG. 2. Mean chain length as a function of the threshold energy  $E_c$  for the simulated systems.  $E_c^* = E_c / \mu^{*2}$ .

of  $N_1$  and  $N_2$  (corresponding to the lowest energy) increase, are closer to each other and closer to the absolute minimum of the dipole-dipole potential, as  $\mu^*$  increases.

Absence of isotropic clustering is also clear from the position of the absolute maximum of  $N_3(E)$ , that occurs at a much higher energy than those of  $N_1$  and  $N_2$ .  $N_3$  has a maximum close to  $-0.25\mu^{*2}$  corresponding to the energy of a head-to-tail configuration at a distance of  $2\sigma$ , i.e., to the energy of third neighbors on a chain.

A quantitative description of the chained structure requires, however, the specification of the threshold energy  $E_c$ . In Fig. 2 we plot  $\bar{N}$  and in Figs. 3(a)–3(c)  $N_m$ ,  $N_{ch}$ , and  $N_{mc}$ , as functions of  $E_c$ . These were calculated from  $N_1(E)$  and  $N_2(E)$ , Eqs. (4,5,6,7) using a simple numerical integration. One obvious criterium for the choice of  $E_c$ , is that which minimizes the dependence of the structure on this choice. Unfortunately, inspection of Figs. 2 and 3(a)–3(c) shows that  $\bar{N}$  and  $N_{mc}$  increase while  $N_m$  decreases with increasing  $E_c$  and thus there is no such  $E_c$ . The number of chains in the system exhibits a maximum corresponding to  $N_1(E) = N_2(E)$ . This is to be expected since all the particles are free monomers if  $E_c = -2\mu^{*2}$  while all particles are in chains if a very large number is chosen for  $E_c$ . Thus the number of chains increases when  $E_c$ , close to  $-2\mu^{*2}$ , increases, and decreases as  $E_c \rightarrow \infty$ , exhibiting one maximum at an intermediate energy. The choice of this value for  $E_c$  corresponds to maximizing the number of chains and there is no reason why we should do this. Clearly the quantitative description of the chainlike structure of the DHS fluid depends on the choice of  $E_c$ , but there appears to be no obvious preferred choice. A similar exercise has been carried out using a definition of chain via a distance criterium [4,5], which requires the specification of a distance  $r_c$ . The conclusions are similar to those for the energetic criterium.

$N_3(E)$ , in Figs. 1(a)–1(c), tends to zero rapidly as  $E \rightarrow -2\mu^{*2}$ . In fact,  $N_3(E) = 0$  for energies less than  $E \approx -1.5\mu^{*2}$ . If  $N_3(E_c) \neq 0$ , we may account for branching, since there is at least one particle with the three lowest energies of interaction less than  $E_c$ . Our theoretical ap-

proach assumes that chains are linear and inspection of  $N_1(E)$ ,  $N_2(E)$ , and  $N_3(E)$  indicates that there is a range of  $E_c$  consistent with this hypothesis. In Table I, we list the number of free monomers and mean chain length calculated using Eqs. (4,5,7) for different threshold energies,  $E_c$ , all of which are consistent with the neglect of branching. The structural parameters are more sensitive to  $E_c$  for stronger dipole moments.

Given a value of  $E_c$ , the equilibrium distribution of chain lengths is calculated. In Fig. 4(a)–4(c) we plot the distributions for the three dipole moments and two threshold energies:  $E_c, E_c = -1.4\mu^{*2}$  and  $E_c = -1.5\mu^{*2}$ . These figures are discussed in more detail in the next section where the simulations are compared with theoretical results.

### III. THEORY FOR THE DIPOLAR HARD SPHERE FLUID: COMPARISON WITH SIMULATIONS

The simulations of [4] revealed that the self-assembled chains, characterizing low density dipolar fluids, break up and recombine during typical equilibrium runs. In living polymer systems, monomers react (join a polymer chain or become free) in dynamical (chemical) equilibrium. Changes in temperature affect the degree of polymerization and the mean chain length of the distribution. This suggests that the dipolar fluid may be considered as a weakly-interacting mixture of chains of all lengths [11–13]. In the following paragraphs we derive the free energy of the ideal mixture of chains (introduced with limited discussion in [11–13]). Consider a system of  $N$  monomers in volume  $V$ , assembled as noninteracting chains of length  $i = 1 \dots N$ . If  $M_i$  is the number of chains of length  $i$ , the partition function is

$$Z = \prod_{i=1}^N \frac{q_i^{M_i}}{M_i!}, \quad (8)$$

where  $q_i$  is the partition function of a chain with  $i$  monomers. The number of monomers is conserved and thus

$$N = \sum_{i=1}^N i M_i. \quad (9)$$

In the thermodynamic limit, the Helmholtz free energy density  $f$  can be derived from Eq. (8), obtaining

$$\beta f = \sum_{i=1}^{\infty} \rho_i (\ln \rho_i - 1 - \ln \tilde{q}_i), \quad (10)$$

where  $\rho_i = M_i/V$  and  $\tilde{q}_i = q_i/V$ . In this limit, the constraint (9) becomes

$$\rho = \sum_{i=1}^{\infty} i \rho_i. \quad (11)$$

From Eq. (10) the chemical potential of species  $i$ , i.e., of chains of length  $i$ , is derived straightforwardly and is found to be

$$\beta \mu_i = \ln \rho_i - \ln \tilde{q}_i. \quad (12)$$

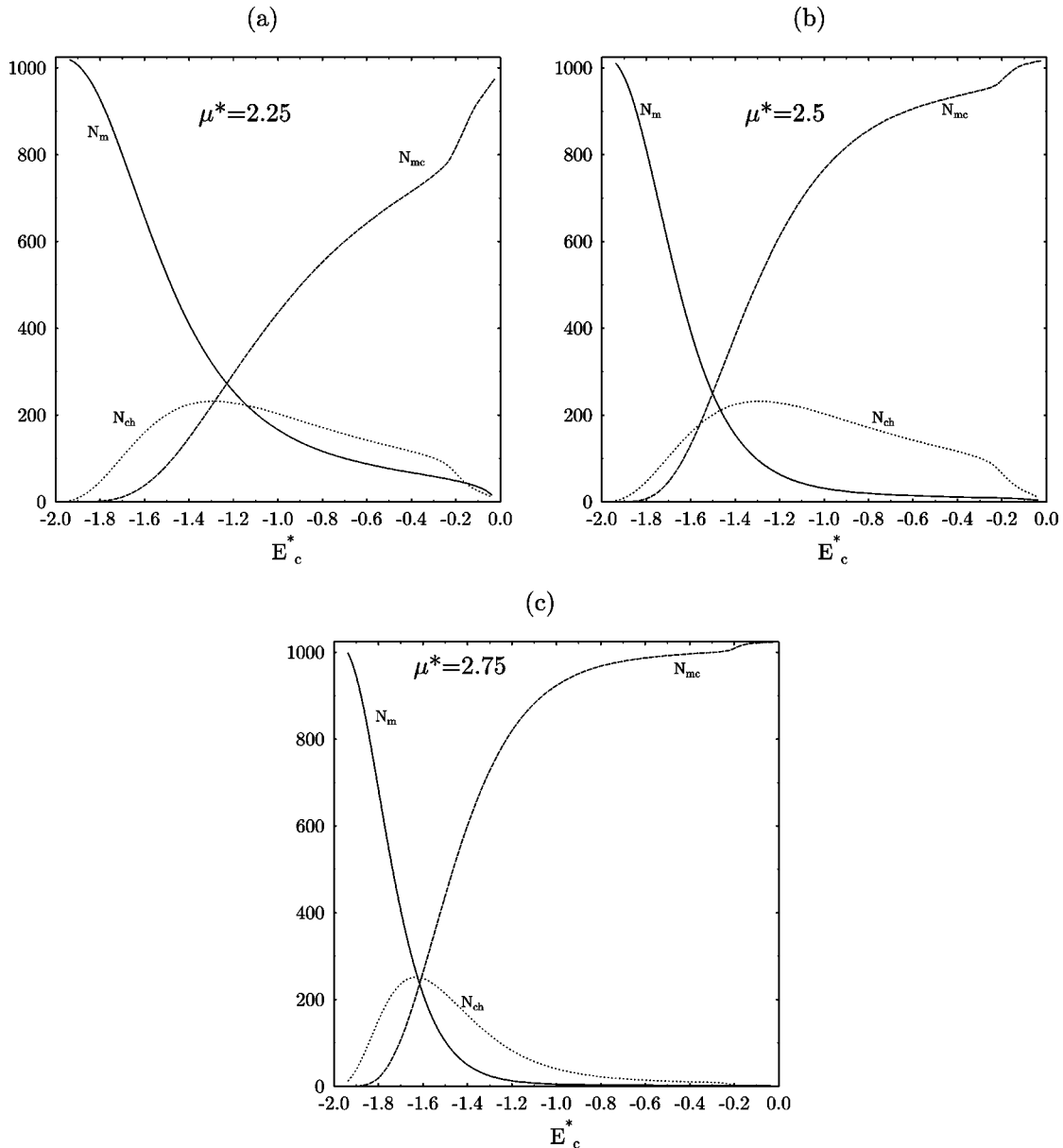
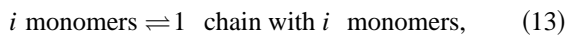


FIG. 3. Number of free monomers  $N_m$ , number of chains  $N_{ch}$ , and number of monomers in the middle of chains, as a function of the threshold energy for the simulated systems.  $E_c^* = E_c / \mu^{*2}$ . (a)  $\mu^* = 2.25$ , (b)  $\mu^* = 2.5$ , (c)  $\mu^* = 2.75$ .

Chemical equilibrium among chains obtains through any chemical reaction that conserves the number of monomers, such as



requiring that the chemical potentials satisfy

$$\mu_i = i \mu_1. \quad (14)$$

Using Eqs. (12) and (14) the density of a chain of length  $i$  is

$$\rho_i = \left( \frac{\rho_1}{q_1} \right)^i \tilde{q}_i. \quad (15)$$

The explicit calculation of the distribution of chain lengths requires an approximation for the partition function of individual chains. The latter may be written as

$$q_i^C = \frac{1}{h^{3i} i!} \int dp^{3i} \exp\left(-\beta \sum_{k=1}^{3i} \frac{p_k^2}{2m}\right) q_i^C, \quad (16)$$

where  $h$  is Planck's constant,  $m$  the mass of a monomer, and  $p^{3i}$  the set of Cartesian coordinates of the linear momenta of the monomers.  $q_i^C$  is the configurational partition function,

$$q_i^C = \int d\vec{r}_1 \dots d\vec{r}_i d\omega_1 \dots d\omega_i \times \exp[-\beta \phi(\vec{r}_1, \dots, \vec{r}_i, \omega_1 \dots \omega_i)], \quad (17)$$

with  $\vec{r}_k$  the position vector of a dipolar hard sphere in the chain and  $\omega_k$  the set of angles that describe the orientation of the dipole.  $\phi$  is the sum of the potential (1) between all pairs of spheres in the chain. Integrating the momenta in Eq. (16) we find for the partition function of a chain,

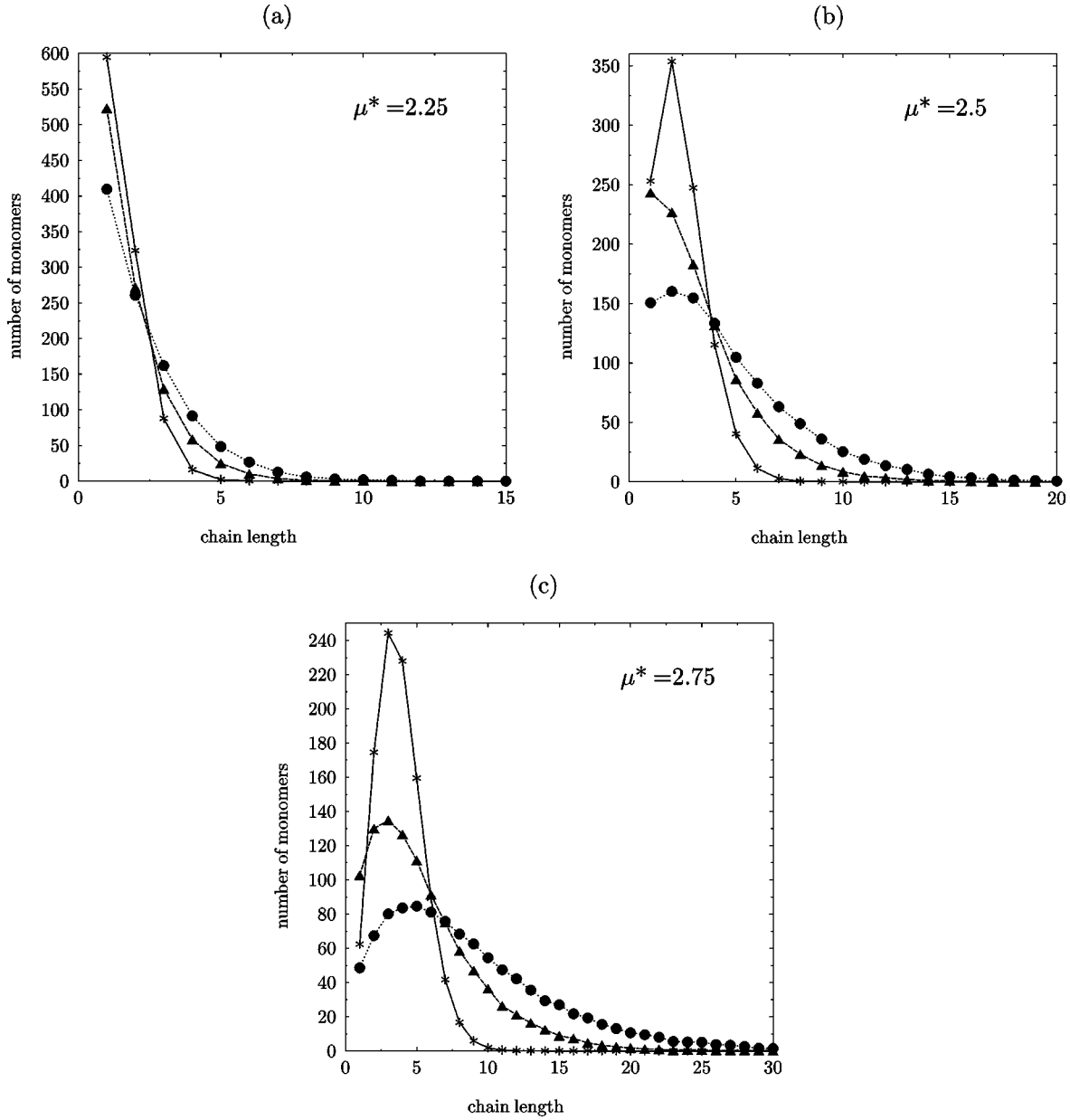


FIG. 4. Number of monomers in chains as a function of chain length (unnormalized chain length distribution). Triangles, simulations with  $E_c = -1.5\mu^{*2}$ ; circles, simulations with  $E_c = -1.4\mu^{*2}$ ; asterisks, theoretical results from (22). (a)  $\mu^* = 2.25$ , (b)  $\mu^* = 2.5$ , (c)  $\mu^* = 2.75$ .

$$q_i = \left(\frac{q_1}{V}\right)^i \frac{q_i^C}{i!}, \quad (18)$$

with  $q_1 = V/\lambda^3$  and  $\lambda$  the de Broglie wavelength of a monomer.

We proceed by calculating  $q_i^C$ , using an approximate method that is valid for short-range interactions in the limit of strong dipoles, i.e., for long chains [12]. We substitute the dipole-dipole interaction in Eq. (17) by a sum of pair potentials between nearest neighbors and write  $q_i^C$  as

$$q_i^C = \int d\vec{r}_1 \dots d\vec{r}_i d\omega_1 \dots d\omega_i \times \exp\left(-\beta \sum_{j=1}^{i-1} \phi_{DHS}(\vec{r}_j - \vec{r}_{j+1}, \omega_j, \omega_{j+1})\right). \quad (19)$$

The integrations in Eq. (19) are carried out using standard methods in the theory of semiflexible polymers and are described in detail in [12]. The result is

$$q_i^C = V \exp[(i-1)S_0], \quad (20)$$

where  $S_0$ , the free energy of a bond (divided by  $-k_B T$ ), is given by [14]

$$S_0 = 2\mu^{*2} + \ln\left(\frac{\pi\sigma^3}{24\mu^{*6}}\right) - \frac{3}{2\mu^{*2}}. \quad (21)$$

Substituting Eqs. (20) and Eq. (18) in (15), we obtain for the density of chains of length  $i$

$$\rho_i = \rho_1^i \frac{\exp[(i-1)S_0]}{i!}. \quad (22)$$

TABLE II. Number of free monomers  $N_m$  and mean chain length  $\bar{N}$  obtained by simulation for several choices of the threshold energy  $E_c$  (see text). Theoretical results obtained using Eqs. (23) and (24) and the corresponding expressions from [12].

$\mu^*$	2.25		2.5		2.75	
	$N_m$	$\bar{N}$	$N_m$	$\bar{N}$	$N_m$	$\bar{N}$
	Simulations					
$E_c = -1.4\mu^{*2}$	410	1.61	155	2.68	50	4.79
$E_c = -1.5\mu^{*2}$	523	1.41	249	2.08	104	3.23
$E_c = -1.6\mu^{*2}$	656	1.25	393	1.62	213	2.22
$E_c = -1.7\mu^{*2}$	800	1.13	591	1.32	407	1.59
	Theory					
This work	594	1.30	253	1.86	62	2.98
[12]	405	1.59	275	2.93	26	7.3

The distribution function  $\rho_i$  depends on the translational partition function through the factorial  $i!$ , which differs from other works on dipolar chains [11,12,15], surfactant systems [16] and living polymers [17]. The translational partition function of the aggregates is usually neglected (set to 1) and the inclusion of this factor is not discussed in the literature (with the exception of [15]). If the chains (or, more generally, the aggregates) are solidlike, then this factor does not appear in the distribution function since the monomers are distinguishable. The assumption of solid aggregates may be correct for the simulations of living polymers on a lattice [17] and for dipolar fluids in strong applied magnetic fields [15] (that induce freezing of the DHSs in columns, aligned in the direction of the field). However, this assumption does not seem to be reasonable for the dipolar hard sphere fluid, since simulations have shown [4] that the spheres diffuse through all the chains in the course of equilibrium runs. Thus we have accounted for the internal energy of bonds as in [12] and added the loss of entropy caused by the indistinguishability of the monomers. Shorter equilibrium chains are then expected to self-assemble.

Substituting Eq. (22) in (11) we obtain for the total density of spheres,

$$\rho = \rho_1 \exp(\rho_1 e^{S_0}). \quad (23)$$

The density of monomers  $\rho_1$ , is calculated through this relation, for a given  $\rho$  and  $\mu^*$ , and using again Eq. (22) the equilibrium chain distribution is determined. The mean chain length  $\bar{N}$  defined as

$$\bar{N} = \frac{\sum_{i=1}^{\infty} i \rho_i}{\sum_{i=1}^{\infty} \rho_i} = \frac{\rho}{\sum_{i=1}^{\infty} \rho_i}, \quad (24)$$

is easily calculated from Eqs. (22) and (23) and is found to be

$$\bar{N} = \frac{\rho e^{S_0}}{\exp(\rho_1 e^{S_0}) - 1}. \quad (25)$$

In Table II we collect the results of the simulations for the

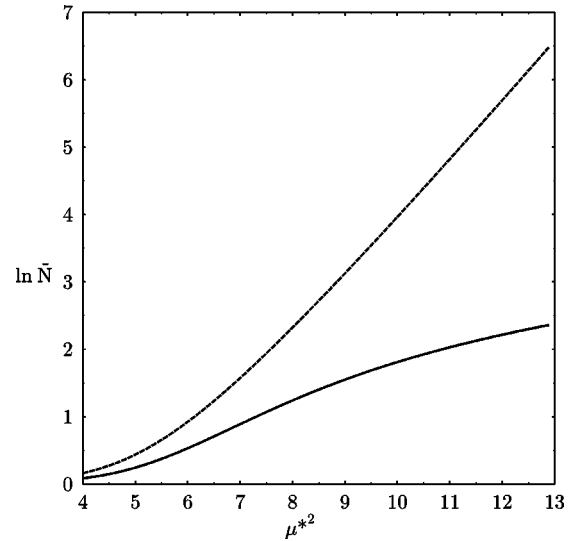


FIG. 5. Comparison of the theoretical results of this work (25) (full line) with those of [12] (dashed line) for the mean chain length  $\bar{N}$  as a function of  $\mu^*$ , at  $\rho^* = 0.05$ . The scale is chosen to exhibit the exponential dependence of the result of [12] on  $\mu^{*2}$ , for high dipole moments.

number of free monomers and for the mean chain length for three values of  $\mu^*$  and four threshold energies. We have also included the results from the theory described in this section and from that of [12]. These results indicate that reasonable agreement is found for  $\mu^* = 2.25$  and  $\mu^* = 2.5$  if the threshold energy is,  $E_c = -1.5\mu^{*2}$ . For the highest value of the dipole moment, the choice of threshold  $E_c = -1.5\mu^{*2}$  yields good agreement for the mean chain length, but agreement for the number of monomers requires  $E_c = -1.4\mu^{*2}$ .

In Figs. 4(a)–4(c) the equilibrium (unnormalized) chain distribution function obtained from Eq. (22) is compared with simulation results. Inspection of the figures clearly shows that the theory underestimates the number of long chains and that this difference becomes more pronounced for the highest values of the dipole moment.

Finally, in order to check quantitatively the effect of the indistinguishability in Eq. (22), we compared the results of Eq. (25) with those of [12] for the mean chain length (Fig. 5). We confirmed that the growth of chains with the dipolar strength is much slower within the present theory. However, a comparison of theories and simulation for other values of the density and dipole moment [5] (see Table III) shows that the inclusion of this factor eliminates the discrepancies, in order of magnitude, for systems with strong dipoles found in previous work [12]. For the lowest density and highest dipole moment (where the theory is expected to hold [12]) the present theoretical results are in quantitative agreement with simulation, while the results of [12] differ markedly.

#### IV. CONCLUSIONS

We have carried out extensive MC simulations of DHS fluids at low density, in order to investigate quantitatively the structure of the fluid in the regime of chainlike correlations. At present, the only practical way to quantify the many-body spatial and orientational correlations that characterize the low density phase of strongly dipolar fluids is through the

TABLE III. Mean chain length: comparison of the theoretical results of this work, those from [12] and the simulations of [5].  $\rho^*$  is the reduced density and  $\mu^*$  the reduced dipole moment, as defined in the text.

$\rho^*$	$\mu^*$	$\bar{N}$ [5]	$\bar{N}$ [12]	$\bar{N}$
0.3	2.0	2.7	1.94	1.36
0.3	2.5	5.2	7.09	2.79
0.3	3.0	16.5	60.0	6.19
0.3	3.5	27.0	966	11.2
0.2	3.5	24.6	789	10.8
0.1	2.0	2.6	1.43	1.16
0.1	2.5	6.7	4.36	2.18
0.1	3.0	24.5	34.8	5.27
0.1	3.5	24.2	558	10.2
0.05	3.5	30.4	395	9.57
0.02	2.0	2.3	1.11	1.04
0.02	3.5	8.4	250	8.75

evaluation of the equilibrium distribution of chains that describes (approximately) the structure of the system. The definition of chains during MC runs, however, raises some questions that have been discussed in detail.

On the theoretical side we have improved the theory of noninteracting self-assembling dipolar chains proposed by [12] by considering that the monomers are indistinguishable.

We have shown that, for the lowest density and highest dipole moment (where the theory is expected to hold) the present theoretical results are in quantitative agreement with earlier simulations, while the results of [12] predict chains that are too long by about one order of magnitude. The remaining differences between the theoretical and simulation results may be traced to an overestimate of the theoretical internal energy (owing to the assumption that the long-range dipolar interactions may be neglected beyond nearest neighbors) and/or to a large correction to the leading term of  $S_0$  for short chains. Interactions between chains are expected to be small at these rather low densities.

We conclude that the chain description is a useful tool to characterize the structure of strongly dipolar fluids, at low density, and that a simple living polymer theory is capable of describing semiquantitatively the structure of a system exhibiting strongly anisotropic many-body correlations.

#### ACKNOWLEDGMENTS

We thank D. Levesque for his interest in this work and for advice. J.M.T. acknowledges the kind hospitality of the Laboratoire de Physique Théorique et Hautes Energies where part of this work was carried out, and the support of the Fundação para a Ciência e a Tecnologia (FCT) through Grant No. PRAXIS XXI/BD/2818/94. J.M.T. and M.M.T.G. acknowledge the FCT for partial support through a running grant and Project No. PRAXIS XXI/2.1/FIS/181/94.

- 
- [1] M.J. Stevens and G.S. Grest, Phys. Rev. Lett. **72**, 3686 (1994).  
[2] M.J. Stevens and G.S. Grest, Phys. Rev. E **51**, 5962 (1995).  
[3] M.J. Stevens and G.S. Grest, Phys. Rev. E **51**, 5976 (1995).  
[4] D. Levesque and J.J. Weis, Phys. Rev. E **49**, 5131 (1994).  
[5] J.J. Weis and D. Levesque, Phys. Rev. Lett. **71**, 2729 (1993).  
[6] J.J. Weis and D. Levesque, Phys. Rev. E **48**, 3728 (1993).  
[7] D. Wei and G.N. Patey, Phys. Rev. Lett. **68**, 2043 (1992); J.J. Weis, D. Levesque, and G.J. Zarragoicoechea, *ibid.* **69**, 913 (1992).  
[8] M.E. van Leeuwen and B. Smit, Phys. Rev. Lett. **71**, 3991 (1993).  
[9] S. Klapp and F. Forstmann, Europhys. Lett. **38**, 663 (1997); S. Klapp and F. Forstmann, J. Chem. Phys. **106**, 9742 (1997).  
[10] B. Groh and S. Dietrich, Phys. Rev. E **50**, 3814 (1994).  
[11] R. van Roij, Phys. Rev. Lett. **76**, 3348 (1996).  
[12] M.A. Osipov, P.I.C. Teixeira, and M.M. Telo da Gama, Phys. Rev. E **54**, 2597 (1996).  
[13] J.M. Tavares, M.M. Telo da Gama, and M.A. Osipov, Phys. Rev. E **56**, R6252 (1997); **57**, 7367(E) (1998) (erratum).  
[14] The factor 24 in Eq. (21) corrects the result of [12].  
[15] P. Jordan, Mol. Phys. **25**, 961 (1973); P. Jordan, *ibid.* **38**, 769 (1979).  
[16] M. Cates and S. Candau, J. Phys.: Condens. Matter **2**, 6869 (1990).  
[17] Y. Rouault and A. Milchev, Phys. Rev. E **51**, 5905 (1995).